Author's Accepted Manuscript

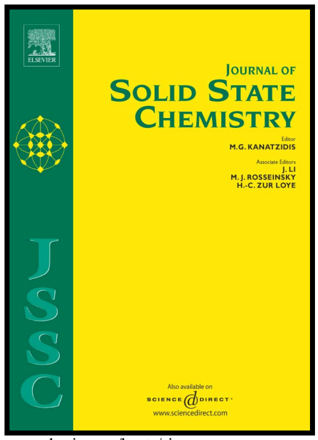

www.elsevier.com/locate/yjssc

Structure and decomposition of the silver formate $Ag(HCO_2)$

Anna N. Puzan, Vyacheslav N. Baumer, Pavel V. Mateychenko

PII: S0022-4596(16)30460-1
DOI: http://dx.doi.org/10.1016/j.jssc.2016.11.022
Reference: YJSSC19603

To appear in: *Journal of Solid State Chemistry*

Cite this article as: Anna N. Puzan, Vyacheslav N. Baumer and Pavel V. Mateychenko, Structure and decomposition of the silver formate $Ag(HCO_2$ *Journal of Solid State Chemistry,* http://dx.doi.org/10.1016/j.jssc.2016.11.022

Structure and decomposition of the silver formate $Ag(HCO_2)$

Anna N. Puzan*, Vyacheslav N. Baumer, Pavel V. Mateychenko

STC ''Institute for Single Crystals'', National Academy of Science of Ukraine, 60 Nauky ave., Kharkiv 61001, Ukraine

Abstract. Crystal structure of the silver formate $Ag(HCO_2)$ has been determined (orthorhombic, sp.gr. P*ccn*, *a*=7.1199(5), *b*=10.3737(4), *c*=6.4701(3)Å, V=477.88(4) Å^3, Z=8). The structure contains isolated formate ions and the pairs Ag_2^{2+} which form the layers in (001) planes (the shortest Ag–Ag distances is 2.919 in the pair and 3.421 and 3.716Å between the nearest Ag atoms of adjacent pairs). Silver formate is unstable compound which decompose spontaneously *vs* time. Decomposition was studied using Rietveld analysis of the powder diffraction patterns. It was concluded that the diffusion of Ag atoms leads to the formation of plate-like metal particles as nuclei in the (100) planes which settle parallel to (001) planes of the silver formate matrix.

Keywords: silver formate, crystal structure, Ag–Ag pairs, layered structure, decomposition, formation of metal phase

Introduction. Silver formate $Ag(HCO_2)$ (hereafter **I**) is a remarkable chemical compound and a precursor of metallic silver. The state of metallic silver obtained from decomposition of (**I**) can be varied within wide limits depending on the method of its production and further processing. Thus, if aqueous solutions of silver nitrate $AgNO_3$ and ammonium formate NH_4COOH are used to obtain the precipitate (**I**), the resulting fine crystalline product may provide both porous and compact silver particles [1] depending on the method of drying. If the synthesis of (**I**) is carried out in the polyethyleneimine (PEI) hydrogel, microporous silver of colloidal dispersion degree [2] can be obtained as a result of decomposition and

*Corresponding author, e-mail: anna_puzan@mail.ru

calcinations of the product. It is also known that decomposition of (I) is an autocatalytic reaction in which the resulting metallic silver catalyzes formic acid decomposition [3,4]. When heated up to ~ 368K (**I**) explodes [5] to form metallic silver, hydrogen and carbon dioxide. If the explosion is of a detonating type, it is accompanied by the formation of fractal clusters of silver in the form of sintered spheric agglomerates [6]. It is known that silver catalysts are most important in industrial applications such as oxidation of methanol to methyl formate [7], (**I**) is used to produce formic acid ether. Salt formation reaction (**I**) may also be used to produce photothermographic composition [8] and to increase the speed of photoelectron emission by doping silver halide with formate ions [9].

In due course, a lot of authors have studied silver particles morphology, kinetics and methods of its forming. Methods of producing silver powder of the expected density have been studied [10]. Nanosilver is used in the synthesis of over-branched polyesters [11]. The process of silver nanoparticles formation with no reducing agents [12] has been studied. It has been found that the shape and size of the resulting silver particles are dependent on the concentration of surfactant, the initial reagents, synthesis temperature and time [13-19], green synthesis of silver nanoparticles is also of considerable interest [20-24]. The kinetics of silver nanoparticles growth in a variety of surface-active solutions has been studied [25]. It has been found that silver clusters obtained under vacuum dehydration in the zeolite channels and networks are photosensitive which allows to use those clusters as photocatalysts in solar cells [26] as well as catalyst [27,28] and practical antimicrobial activity [21,29]. The unique properties of silver produced in this way are proved by the fact that CO_2 recovery rate is twice as high on Ag (110) than on Ag (111) and Ag (100) [30].

Furthermore, (**I**) is commonly used for silver plating and obtaining of biologically active materials [21, 31]. All the above-mentioned suggests that the silver formate is an important precursor for the particulate metallic silver. As its crystalline structure has not yet been described, one of the aims of the present study is to determinate and analyze it. As noted above, silver formate is an unstable compound and the process of its expansion in the solutions and dispersed media was studied by many authors, but the decomposition of pure bulk silver formate has not been described, and it is the second aim of the present work.

1. Experimental

Since methods of obtaining of silver formate from solutions lead to formation of the disperse product that rapidly decays, they cannot be used to obtain crystals for X-ray study. To obtain crystals suitable for the study we used a technique similar to the one described in [32]. Silver carbonate precipitate Ag_2CO_3 was obtained by pouring together the stoichiometric amounts of $AgNO_3$ (>99% purity, 0.75mol/1) and NH_4HCO_3 (analytical grade, 1mol/1) solutions at 320K, washed with distilled water, filtered and dried. Obtained yellow powder was developed with concentrated formic acid (the 5**%** excess of formic acid as compared with stoichiometric quantity was added to the powder). At the end of CO_2 gas evolution, the formation of colorless crystals which quickly colored in yellow and further more slowly black was observed in the solution.
The obtained particles of (**I**) are shown in Figure 1a,b (JEOL JSM-6390LV X-max raster electron microscope).

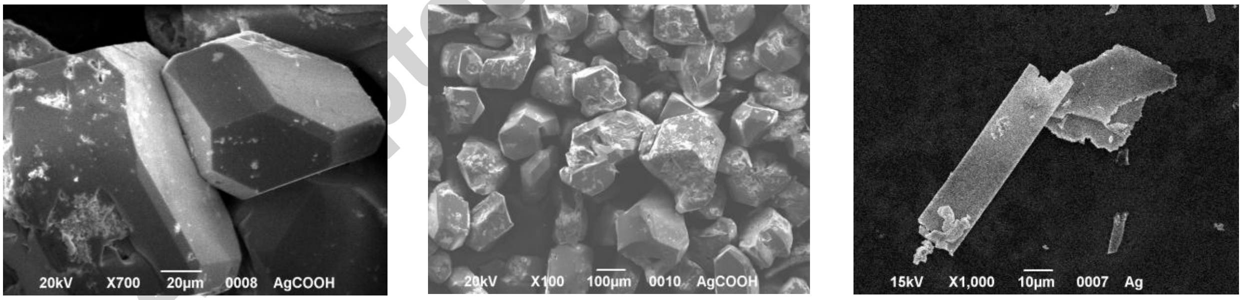

a b c

Figure 1. REM photographs: a,b – the silver formate crystals; c – plate-like silver particles after decomposition.

Fresh-precipitated crystals of (**I**) were used for X-ray diffraction study using the "Xcalibur3" automated single-crystal diffractometer (Oxford Diffraction Ltd.), monochromated MoKα radiation, "Sapphire3" CCD detector. The structure was solved by direct methods and refined by the least squares ("SHELX97" program package [33]) in the anisotropic approximation (hydrogen atom was refined isotropically). Main crystal data and refinement results are given in Table 1. Full data for the structure (**I**) have been deposited with the ICSD Database, CSD–431932. Copie of this information may be obtained at http://www.fiz-karlsruhe.de/obtaining_crystal_structure_data.html.

The rest of silver formate obtained was used for the X-ray powder analysis (Bragg-Brentano diffractometer "Siemens D500", CuKα-radiation, curved graphite monochromator on the diffracted beam, point scintillation detector, instrumental profile parameters from LaB_6 pattern used as external standard, $10^o<2\theta<90^o$, $\Delta 2\theta=0.02°$, dwell time of 5 sec. per point) using the Rietveld method (WinPlotr&FullProf program [34]). Initially the qualitative separation of the size and strain broadening effects on powder pattern of (I) were carried out using Williamson-Hall method [35]. The dependence of integral breath ($\beta_{hkl}\cdot\cos\theta$) for non-overlapped reflections against d_{hkl}^{-1} showed y-intercept and slope simultaneously. Quantitative calculations of these effects were performed using P.W.Stephens' formalism [36] implemented in Fullprof program.

Tabel 1. Crystal data and refinement indices for (**I**)

Empirical formula	$CHAgO_2$
Formula weight, a.m.u.	152.89
Temperature (K)	293(2)
Wavelength (E)	0.71073
Crystal system	Orthorhombic
Space group	*Pccn*
a (E)	7.1199(5)
b (E)	10.3737(4)
c (E)	6.4701(3)
V (E^3)	477.88(4)
Z	8
Calculated density ($g·cm^{-3}$)	4.250
Absorption coefficient (mm^{-1})	8.098
F(000)	560
Crystal size (mm)	0.14 Ч 0.12 Ч 0.09
θ range for data collection (є)	3.47 to 36.41
Index ranges	$-6 \le h \le 11$, $-16 \le k \le 16$, $-10 \le l \le 5$
Reflections collected / unique	2224 / 1038 (R_{int} = 0.0191)
Completeness to 2θ (35є)	95.1%
Max. and min. transmission	0.5294 and 0.3969
Refinement method	Full-matrix least-squares on F^2
Data / parameters	1063 / 42
Goodness-of-fit on F^2	0.977
Final R indices [I>2σ(I)]	R_1 = 0.0283, wR_2 = 0.0320
R indices (all data)	R_1 = 0.0586, wR_2 = 0.0383
Extinction coefficient	0.0028(2)
Largest diff. peak and hole ($e.E^{-3}$)	0.671 and -0.672

2. Discussion

2.1.**Crystal Structure**

The main feature of the structure (**I**) is the presence of the bond metal-metal (Ag-Ag of 2.919Å), indicating the presence of a cluster Ag_2^{2+}. This interaction is described in the literature as the “argentophilic interaction” [37]. Each cluster is environed with the six formate ions, and each formate-ion is enclosed with six Ag_2

clusters (Figure 2). Each silver atom in the cluster is co-ordinated by four oxygen atoms, belonging to four formate ions, two of which are bridged between the atoms of the same Ag-cluster with Ag-O distances of 2.32, 2.28Å. The remaining oxygen atoms are those of formate ions being bridged between adjacent clusters, Ag-O distances of 2.52, 2.47Å (Table 2) being characteristic for them.

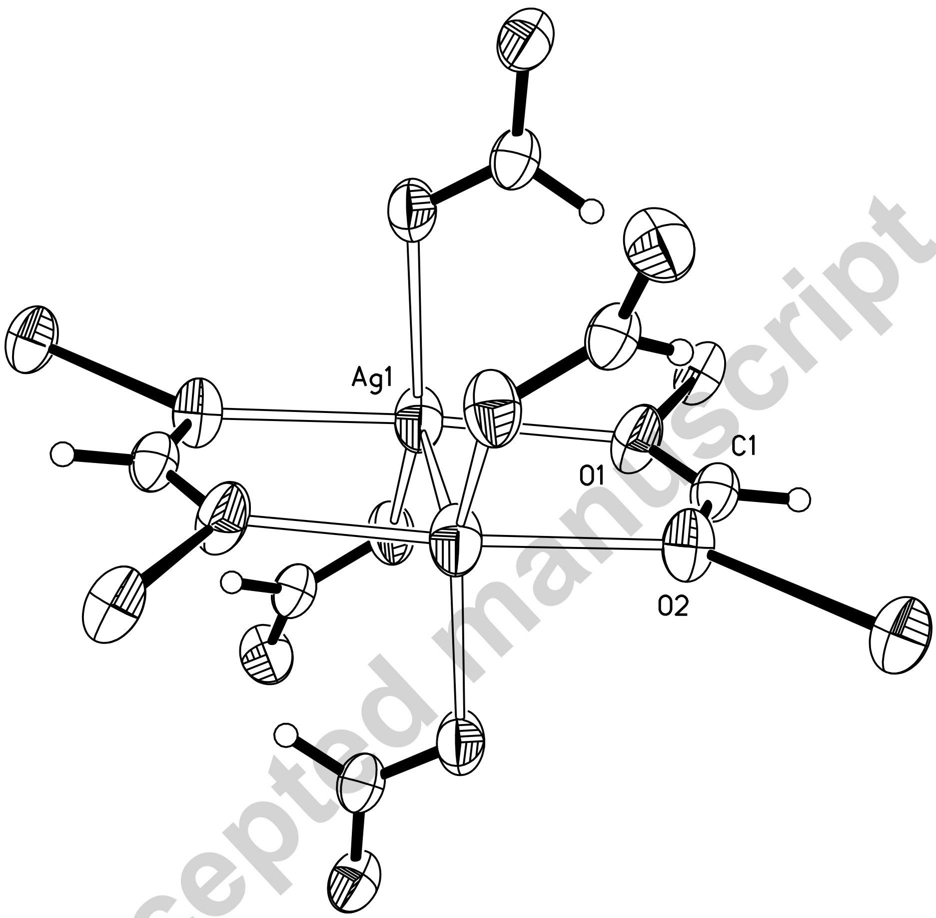

Fig.2. Atomic numbering scheme and thermal ellipsoids for (**I**). Symmetrically equivalent atoms are not denoted.

Table 2.Bond lengths (Å) and angles (º)

Ag(1)-O(1)	2.2830(17)	Ag(1)-Ag(1)#1	2.9176(5)	O(2)-Ag(1)#1	2.3171(16)
Ag(1)-O(2)#1	2.3171(16)	O(1)-C(1)	1.236(3)	O(2)-Ag(1)#5	2.4671(18)
Ag(1)-O(2)#2	2.4671(18)	O(1)-Ag(1)#4	2.5168(19)	C(1)-H(1)	0.95(2)
Ag(1)-O(1)#3	2.5168(19)	O(2)-C(1)	1.259(3)		

O(1)-Ag(1)-O(2)#1	161.87(6)	C(1)-O(1)-Ag(1)	135.02(18)
O(1)-Ag(1)-O(2)#2	100.45(6)	C(1)-O(1)-Ag(1)#4	122.25(16)
O(2)#1-Ag(1)-O(2)#2	93.04(4)	Ag(1)-O(1)-Ag(1)#4	101.35(7)
O(1)-Ag(1)-O(1)#3	91.74(6)	C(1)-O(2)-Ag(1)#1	115.75(16)
O(2)#1-Ag(1)-O(1)#3	81.11(6)	C(1)-O(2)-Ag(1)#5	114.05(15)
O(2)#2-Ag(1)-O(1)#3	153.54(7)	Ag(1)#1-O(2)-Ag(1)#5	130.12(8)
O(1)-Ag(1)-Ag(1)#1	74.59(5)	O(1)-C(1)-O(2)	126.3(2)
O(2)#1-Ag(1)-Ag(1)#1	87.71(5)	O(1)-C(1)-H(1)	115.8(13)
O(2)#2-Ag(1)-Ag(1)#1	125.93(5)	O(2)-C(1)-H(1)	117.8(14)
O(1)#3-Ag(1)-Ag(1)#1	79.86(5)		

Symmetry transformations used to generate equivalent atoms:
#1 -x+1,-y+1,-z #2 -x+1,y+1/2,-z+1/2 #3 -x+1/2,y,z-1/2 #4 -x+1/2,y,z+1/2
#5 -x+1,y-1/2,-z+1/2

Crystal structure of (**I**) (3a,b) is a three-dimensional polymer network in which cluster pairs of silver atoms extend along the and directions, the distance between nearest silver atoms of the adjacent pairs is 3.421Å. Thus chains form the layer in the plane (001), the shortest distance Ag...Ag 3.716Å is observed for the chains located in adjacent layers in the (010) plane. The presence of the chains and layers in the structure indicates possible diffusion directions under decomposition of (**I**).

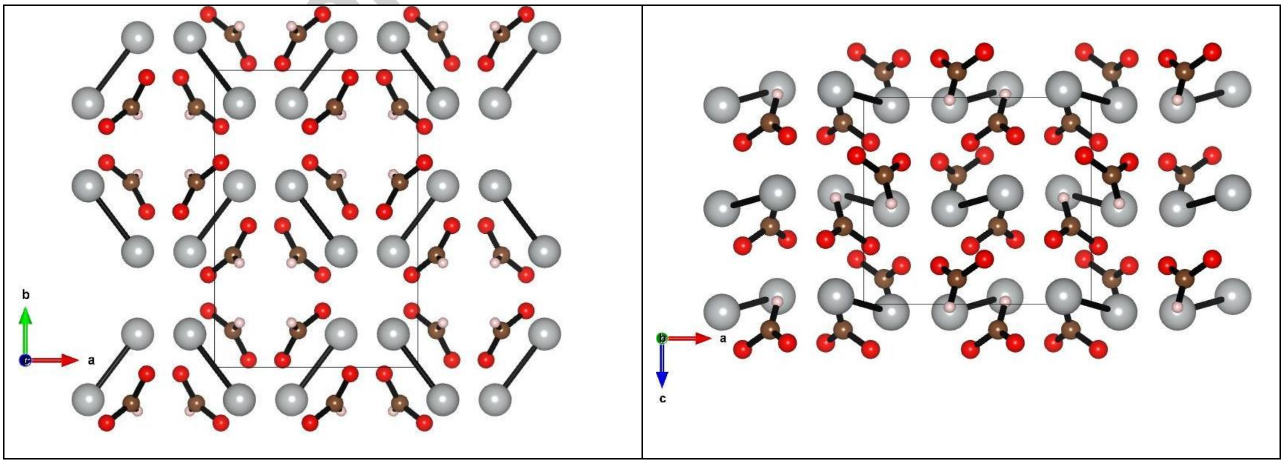

a b

Figure 3a,b. Packing in the structure (**I**), visualized with Vesta software [38]

2.2.**Decomposition**

Silver formate is unstable in the air. It decomposes spontaneously at room temperature to form metallic silver phase. This process was experimentally studied using powder X-ray analysis. Silver formate freshly produced was ground in a mortar and placed in a glass sample holder for X-ray pattern registration, which was repeated after a certain time. The resulting serie of patterns is shown in Figure 4.

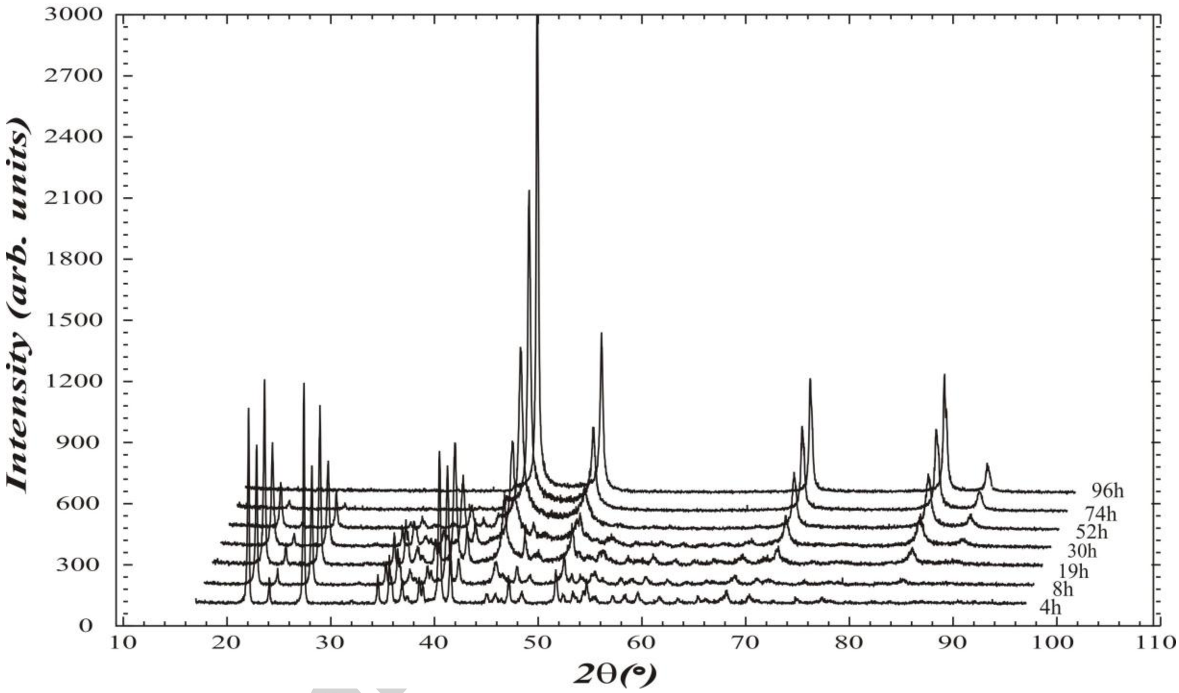

Fig. 4. X-ray powder patterns for the decomposing silver formate

Each pattern obtained was refined by the Rietveld method using anisotropic line broadening approximation, which allows to evaluate the average size of the forming silver particles in different directions. As an example, Figure 5 shows the results of the refinement for the pattern obtained after 14 hours of decomposition.

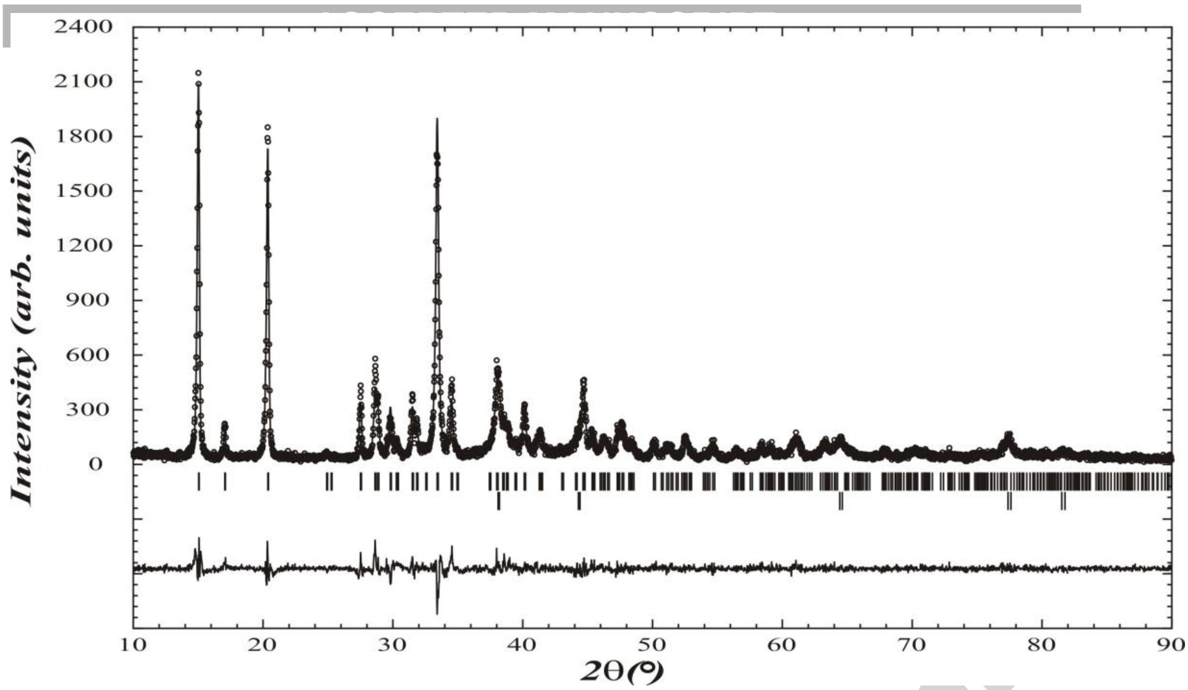

Fig.5. The Rietveld refinement results for the (**I**) after 14h decomposition.

Silver lines in the first pattern are very weak, whole X-ray pattern corresponds to the phase of silver formate. Further on, the increase in the intensity of metallic silver phase lines and the extinction of silver formate phase lines at each successive stage can be observed. And after about 90 hours of exposure the silver formate lines disappear completely, the last X-ray pattern corresponds completely to the formed metallic silver phase.

Results of the Rietveld refinement were used to make the diagrams which reveal dependence of the obtained silver particle size on the time and of the anisotropic particle size on the silver phase percentage (Fig.6a,b).

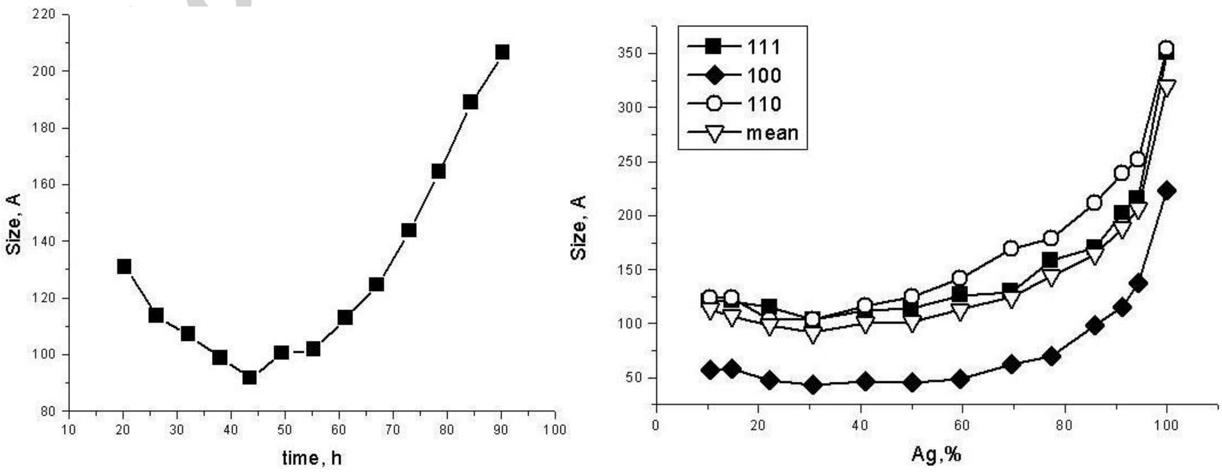

a b

Fig.6. Dependence of the silver particle size on the time of decomposition (a) and anisotropic size of the Ag particles *vs* Ag content (b).

It can be concluded that nuclei of the metal phase are formed at the initial stage of decomposition. The average size of these nuclei decreases on time from 130Å at the beginning to ~ 50Å after 42 hours of decomposition. This decreasing can be explained by the diminution of formate content in the sample and the fact that decaying particles of the salt matrix eventually became spaced by particles of product for which the coalescence and re-crystallization processes are impeded at the room temperature. Further, after about half of the original salt is decomposed, the average size of the silver particles gradually increases because the silver resulting from the formate decomposition crystallizes on the existing nuclei. Defining particle size according to Rietveld method is performed by broadening the lines profile in comparison with the profile of the standard sample, and in the case of silver formate the broadening is not the same for all lines, i.e. is anisotropic, which, in principle, corresponds to the anisotropic size effect. This means that the resulting silver particles have different sizes in different crystallographic planes. For the coordinate plane (100) the average size is essentially smaller than in other crystallographic planes (50 and ~120Å, respectively). This suggests that formed metal particles have a plate-like habitus. On considering the microcrystalline effects in the original matrix of silver formate, it can be noted that the minimum size of the particles during the decomposition is observed for the (100) planes and is of 360-200Å depending on the decomposition time (Fig.7a,b), whereas in the other planes it is noticeably greater. Moreover, just in the (100) planes of the formate matrix are characterized by largest microstrain values (Fig.7). It was mentioned above that the shortest distances 3.715Å of between the cluster silver pairs in the initial formate are observed in the (010) plane. The analysis of microstructural characteristics for the matrix and for the forming silver allows to suggest that during the initial stage of decomposition preferable pair diffusion occurs in the (100) plane of the matrix, originating the formation of silver (100) planes, despite they are not closely packed.

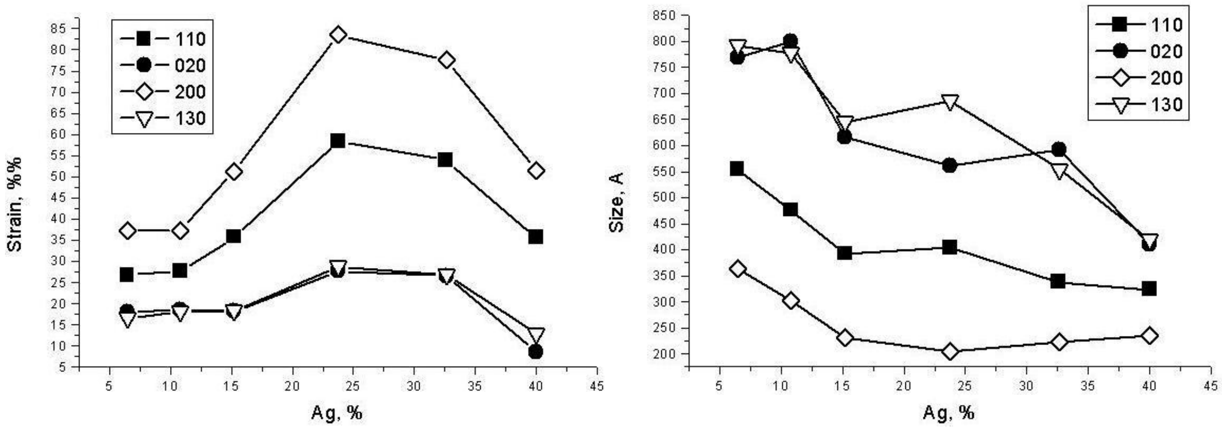

a b

Fig. 7. Microstructural effects in the silver formate matrix (a – microstains, b – anisotropic size).

Acknowledgement.

Authors appreciate the International Centre for Diffraction Data for the financial support (Grants No. 03-02 and 14-01).

[1] H.L. Won, H. Nersisyan, Ch.Wh. Won, J.-M. Lee, J.-S. Hwang, Preparation of porous silver particles using ammonium formate and its formation mechanism, Chemical Engineering J. **156** (2010) 459–464
[2] R.-H. Jin, J.-J. Yuan, Fabrication of silver porous frameworks using poly(ethyleneimine) hydrogel as a soft sacrificial template, J. Mater. Chem. **15** (2005) 4513-4517.
[3] K. Fukuda, T. Onishi, K. Tamaru, Decomposition of Formic Acid on Silver Catalyst Adsorption Measurement during Surface Catalysis, Bull.Chem.Soc.Jap. **42** (1969) 1192-1196.
[4] B.A.Sexton, R.J.Madix, A vibrational study of formic acid interaction with clean and oxygen-covered silver (110) surfaces, Surface Science **105** (1981) 177-195.
[5] V.N. Kolesnikov, The formation of silver fractal aggregate clusters during the thermal decomposition of silver oxalate, Khimicheskaya Fizika (in Russian) **17** (1998) 109-111.
[6] V.N. Kolesnikov, Silvers oxalate and formate thermolysis: forms of metal crystallization in burning and detonating modes, Kharkov University Bulletin. Chemical Series **13** (2005) 145-147.
[7] Z.Yang, J.Li, X. Yang, Y. Wu, Catalytic oxidation of methanol to metyl formate over silver – a new purpose of traditional catalysis system, Catalysis letters **100** (2005) 205-211.
[8] S.E. Sheppard, W. Vanselow, Photothermographic composition, US Patent **1,976,302** (1934).
[9] J. Belloni, Photography: enhancing sensitivity by silver-halide crystal doping, Radiation Physics and Chemistry **67** (2003) 291–296.
[10] O.A. Short, N.J. Metuchen, Silver powder and method for producing same, US Patent **2,752,237** (1956).
[11] Z. Zhu, L. Kai, Y. Wang, Synthesis and applications of hyperbranched polyesters—preparation and characterization of crystalline silver nanoparticles, Materials Chemistry and Physics **96** (2006) 447–453
[12] M. Kim, J.-W. Byun, D.-S. Shin, Y.-S. Lee, Spontaneous formation of silver nanoparticles on polymeric supports, Materials Research Bulletin **44** (2009) 334–338
[13] J. Zhu, S. Liu, O. Palchik, Y. Koltypin, A. Gedanken, Shape-Controlled Synthesis of Silver Nanoparticles by Pulse Sonoelectrochemical Methods, Langmuir **16** (2000) 6396-6399
[14] D. Yu, V. Wing-Wah Yam, Hydrothermal-Induced Assembly of Colloidal Silver Spheres into Various Nanoparticles on the Basis of HTAB-Modified Silver Mirror Reaction, J. Phys. Chem. B **109** (2005) 5497-5503
[15] D. Xiong, H. Li, Colorimetric detection of pesticides based on calixarene modified silver nanoparticles in water, Nanotechnology **19** (2008) 1-6.
[16] Z. Khan, J.I. Hussain, S. Kumar, A.A. Hashmi, M.A. Malik, Silver Nanoparticles: Green Route, Stability and Effect of Additives, J. of Biomaterials and Nanobiotechnology, **2** (2011) 390-399.

[17] G. Tosun, H.D. Glicksman, Process for making finely divided particles of silver metal, US Patent **4,979,985** (1990).
[18] Y. Tan, Y. Li, D. Zhu, Preparation of silver nanocrystals in the presence of aniline, J. of Colloid and Interface Science **258** (2003) 244–251.
[19] J.I. Hussain, S. Kumar, A.A. Hashmi, Z. Khan, Silver nanoparticles: preparation, characterization, and kinetics, Adv. Mat. Lett. **2** (2011) 188-194.
[20] J. Xie, J.Y. Lee, D.I.C. Wang, Y.P. Ting, Silver Nanoplates: From Biological to Biomimetic Synthesis, American Chemical Society **1** (2007) 429–439.
[21] V.K. Sharma, R.A. Yngard, Y. Lin, Silver nanoparticles: Green synthesis and their antimicrobial activities, Advances in Colloid and Interface Science **145** (2009) 83–96.
[22] S.T. Dubas, V.Pimpan, Green synthesis of silver nanoparticles for ammonia sensing, Talanta **76** (2008) 29–33.
[23] P.C. Nagajyothi, S.E. Lee, M. An, K.D. Lee, Green Synthesis of Silver and Gold Nanoparticles Using Lonicera Japonica Flower Extract, Bull. Korean Chem. Soc. **33** (2012) 2609-2612.
[24] Q. Faisal, R. Ahmad, Z. Khan, Bio-conjugated silver nano-materials and shape-directing role of cetyltrimethylammonium bromide, J. of Advances in Chemistry **2** (2013) 57-67.
[25] Z. Khan, S.A. Al-Thabaiti, E.H. El-Mossalamy, A.Y. Obaid, Studies on the kinetics of growth of silver nanoparticles in different surfactant solutions, Colloids and Surfaces B: Biointerfaces **73** (2009) 284–288.
[26] T. Sun, K. Seff, Silver Clusters and Chemistry in Zeolites, Chemical Reviews. **94** (1994) 857-870.
[27] I.E. Wachs, R.J. Radix, Oxidation of methanol on silver (110) catalyst, Surface Science **76** (1978) 531-558.
[28] A.G. Sault, R.J. Madix, Effects of ambient Oxygen on the stability of Formate and Acetate Intermediates on Ag(110), J. Phys. Chem. **90** (1986) 4723-4725.
[29] I. Sondi, B. Salopek-Sondi, Silver nanoparticles as antimicrobial agent: a case study on E. coli as a model for Gram-negative bacteria, Journal of Colloid and Interface Science **275** (2004) 177–182.
[30] A. Salehi-Khojin, H.-R.M. Jhong, B.A. Rosen, W. Zhu, S. Ma, P.J.A. Kenis, R.I. Masel, Nanoparticle Silver Catalysts That Show Enhanced Activity for Carbon Dioxide Electrolysis, J. Phys. Chem. C **117** (2013) 1627−1632.
[31] M.L. Block, A.H. Mones, Electrical conductor material and method of making same, US Patent **3,345,158** (1967).
[32] J.P. Fugassi, G.A. Cowan, Method of making silver formate, US Patent **2,630,444** (1953).
[33] G.M. Sheldrick, A short history of SHELX, Acta Cryst. A **64** (2008) 112-122.
[34] J. Rodriguez-Carvajal, T. Roisnel, FullProf.98 and WinPLOTR New Windows 99/NT Applications for Diffraction, Commission for Powder Diffraction, International Union of Crystallography, Newsletter **20** (1998) 35-36.
[35] G. K. Williamson, W. H. Hall, X-Ray line broadening from filed aluminium and wolfram, Acta Metall. **1** (1953) 22-31.

[36] P. W. Stephens, Phenomenological model of anisotropic peak broadening in powder diffraction, J. Appl. Cryst. **32** (1999) 281-289.
[37] H. Schmidbaur, A. Schier, Argentophilic Interactions, Angew. Chem. Int. **53** (2014) 2-41.
[38] K. Momma, F. Izumi, VESTA 3 for three-dimensional visualization of crystal, volumetric and morphology data, J. Appl. Crystallogr., **44** (2011) 1272-1276.

- Silver formate $Ag(HCO_2)$ was synthesized and characterized
- Layered packing of Ag-Ag pairs in the structure was found
- Decomposition of $Ag(HCO_2)$ and formation of metal phase were studied
- Rietveld-refined micro-structural characteristics during decomposition reveal the space relationship between the matrix structure and forming Ag phase

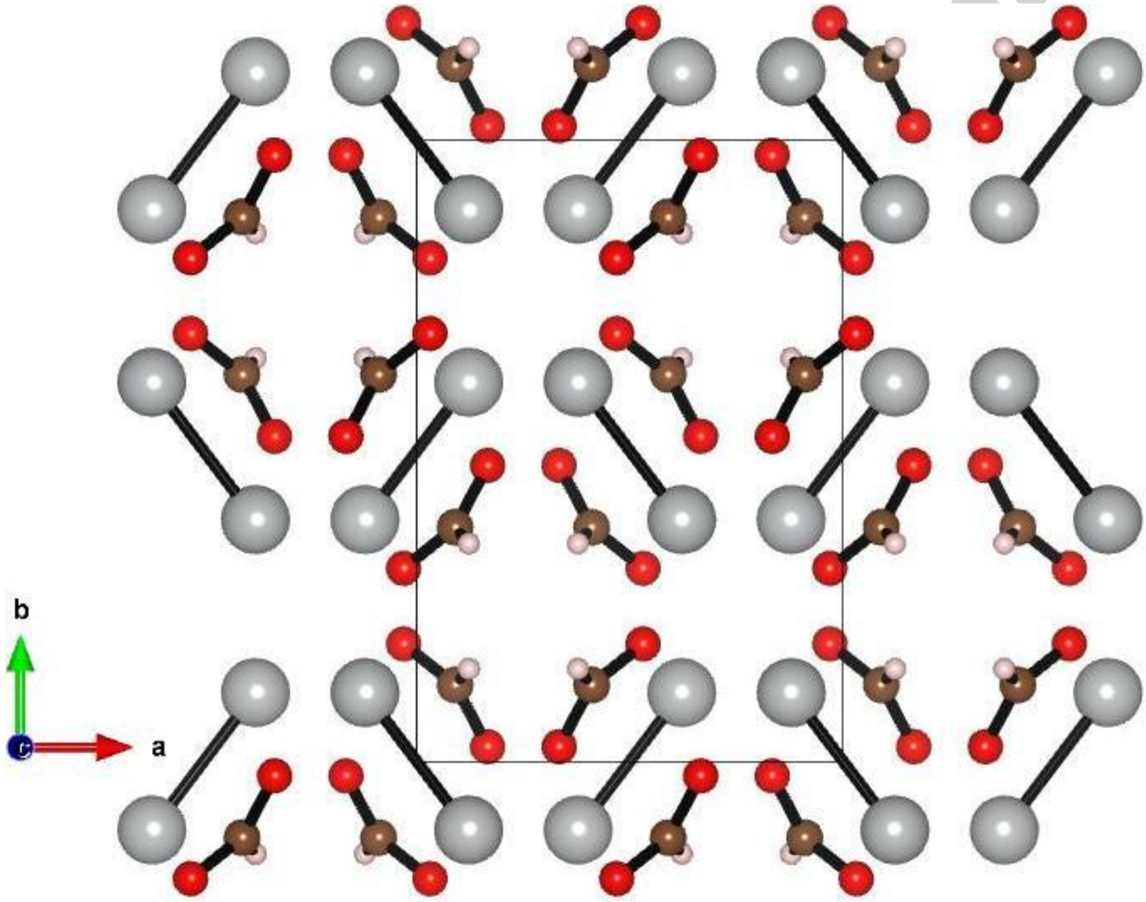

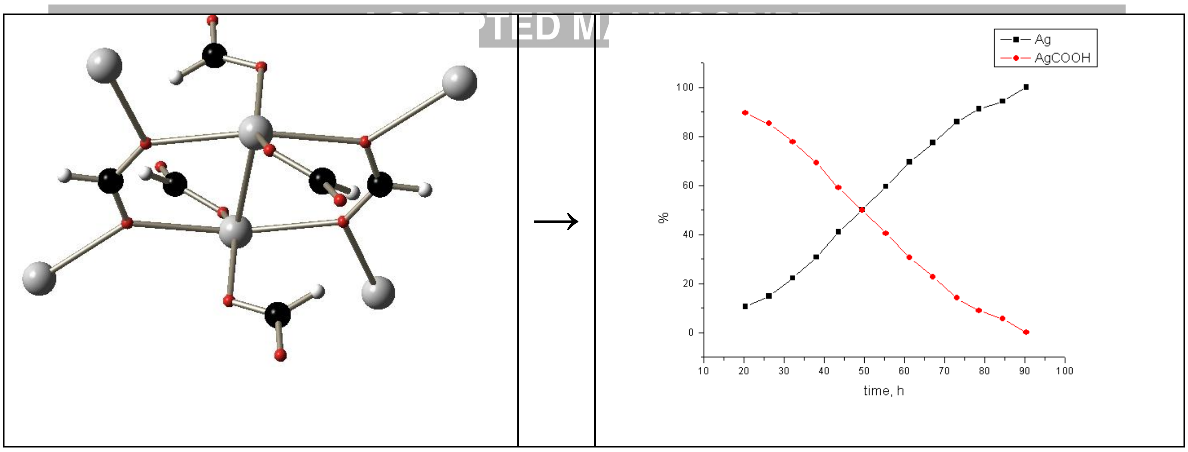
Ag
AgCOOH
%
time, h
0
20
40
60
80
100
10
20
30
40
50
60
70
80
90
100